# Solution Structure of the DNA Methyl Phosphotriester Repair Domain of *Escherichia coli* Ada[†,‡]

Lawrence C. Myers,[§] Gregory L. Verdine,[*,§,∥] and Gerhard Wagner[*,§,⊥]

*Program for Higher Degrees in Biophysics and Department of Chemistry, Harvard University, Cambridge, Massachusetts 02138, and Department of Biological Chemistry and Molecular Pharmacology, Harvard Medical School, Boston, Massachusetts 02115*

*Received August 18, 1993; Revised Manuscript Received October 4, 1993*[⊛]

ABSTRACT: The *Escherichia coli* Ada protein repairs methyl phosphotriesters in DNA by direct, irreversible methyl transfer to one of its own cysteine residues. The methyl-transfer process appears to be autocatalyzed by coordination of the acceptor residue, Cys-69, to a tightly bound zinc ion. Upon methyl transfer, Ada acquires the ability to bind DNA sequence-specifically and thereby to induce genes that confer resistance to methylating agents. The solution structure of an N-terminal 10-kDa fragment of Ada, which retains zinc binding and DNA methyl phosphotriester repair activities, was determined using multidimensional heteronuclear nuclear magnetic resonance techniques. The structure reveals a zinc-binding motif unlike any observed thus far in transcription factors or zinc-containing enzymes and provides insight into the mechanism of metalloactivated DNA repair.

In response to the persistent threat posed by aberrant methylation of DNA, virtually all organisms express proteins that recognize and repair the resulting lesions (Lindahl, 1993). One such protein is *Escherichia coli* Ada, which repairs the mutagenic lesion $O^6$-methylguanine ($O^6$MeG)[1] by direct, irreversible transfer to a cysteine residue in the C-terminal domain. Ada also repairs the $S_p$ diastereomer of DNA methyl phosphotriesters [MeP(s)] by direct transfer to another cysteine residue, Cys-69, located in the N-terminal domain (Demple, 1990) (Figure 1A). Methylation of Cys-69 reveals a sequence-specific DNA binding activity in the N-terminal domain, which enables Ada to activate transcription of a methylation-resistance regulon. The methylated Ada protein activates transcription of the *ada* gene as well as several other genes that encode DNA repair functions. Hence, aside from its direct role in the repair of mutagenic DNA lesions, Ada acts as a chemosensor for methylation damage in the cell (Lindahl et al., 1988).

The N-terminal domain of Ada possesses a tightly bound zinc ion that is necessary for proper folding *in vitro* and *in vivo* (Myers et al., 1992). $^{113}$Cd nuclear magnetic resonance (NMR) studies on Ada fragments revealed an unusual Cys-$X_3$-Cys-$X_{26}$-Cys-$X_2$-Cys ligand arrangement (Myers et al., 1993) reminiscent of, but not identical to, the four cysteine zinc-binding motifs of the nuclear hormone receptor family of transcription factors (Schwabe & Rhodes, 1991). Whereas the majority of eukaryotic transcription factors possess structural zinc, Ada is presently the sole example of such a factor in prokaryotes; this has raised the question of whether Ada is structurally and perhaps evolutionarily related to regulatory proteins found in higher organisms (Berg, 1990). One of the four ligand residues in Ada was identified as Cys-69, thereby implicating the zinc ion not only in stabilization of the protein structure but also in direct metalloactivation of the methyl acceptor residue (Myers et al., 1993) (Figure 1A). The zinc binding and DNA MeP repair functionality is completely retained in a 10-kDa fragment of the N-terminus of Ada (Myers et al., 1992) comprising residues 1–92 (N-Ada10) (Figure 1B). N-Ada10 lacks, however, residues essential for sequence-specific DNA binding (Sakashita et al., 1993). Here we report the structure determination of *E. coli* N-Ada10 by NMR methods.

## MATERIALS AND METHODS

*Production and Purification of N-Ada10.* Unlabeled N-Ada10 protein was expressed and purified as previously described (Myers et al., 1992). The uniformly $^{15}$N-labeled N-Ada10 fragment was obtained by growing the cells in M9-glc minimal medium containing $^{15}NH_4Cl$ (Cambridge Isotopes) as the sole nitrogen source. To obtain the zinc form of N-Ada10, the M9-Glc minimal medium was supplemented with $ZnCl_2$ (100 $\mu$M). The purified protein samples were exchanged into a buffer containing 25 mM sodium phosphate, 50 mM NaCl, and 10 mM 2-mercaptoethanol, pH 6.4, and concentrated to 2–3 mM in protein. The concentrated samples were lyophilized and resuspended in a equal volume of degassed 95% $H_2O$/5% $D_2O$ or $D_2O$ (99.99%) under argon in a 5-mm NMR tube for NMR measurements.

*NMR Spectroscopy.* Measurements were made using 2–3 mM N-Ada10 samples at pH 6.4 and 25 °C. The pH of the $D_2O$ samples was adjusted for the isotope effects. Homonuclear total correlation spectroscopy (TOCSY) (Braunsch-

[†] This work was supported by grants (to G.L.V.) from the Chicago Community Trust (Searle Scholars Program) and the National Science Foundation (Presidential Young Investigator Award Program) and by grants (to G.W.) from the NIH and NSF. L.C.M. is a Howard Hughes Medical Institute Predoctoral Fellow.

[‡] Atomic coordinates have been deposited in the Brookhaven Protein Data Bank under the filename 1ADN.

* To whom correspondence should be addressed.

[§] Program for Higher Degrees in Biophysics.

[∥] Department of Chemistry.

[⊥] Department of Biological Chemistry and Molecular Pharmacology.

[⊛] Abstract published in *Advance ACS Abstracts,* November 15, 1993.

[1] Abbreviations: $O^6$-MeG, $O^6$-methylguanine; MeP, methyl phosphotriester; N-Ada20, Ada fragment containing residues 1–178; C-Ada19, Ada fragment containing residues 179–354; N-Ada10, Ada fragment containing residues 1–92; NMR, nuclear magnetic resonance; M9-Glc, M9 minimal media supplemented with glucose; TOCSY, total correlation spectroscopy; NOESY, nuclear Overhauser effect spectroscopy; HMQC, heteronuclear multiple-quantum coherence spectroscopy; DQF-COSY, double-quantum-filtered correlation spectroscopy; HSQC, 2D $^{15}$N–$^1$H heteronuclear single-quantum coherence spectroscopy; 2D, two dimensional; RMSD, root-mean-square deviation; ADH, alcohol dehydrogenase; ATCase, aspartate transcarbamoylase.

0006-2960/93/0432-14089$04.00/0 

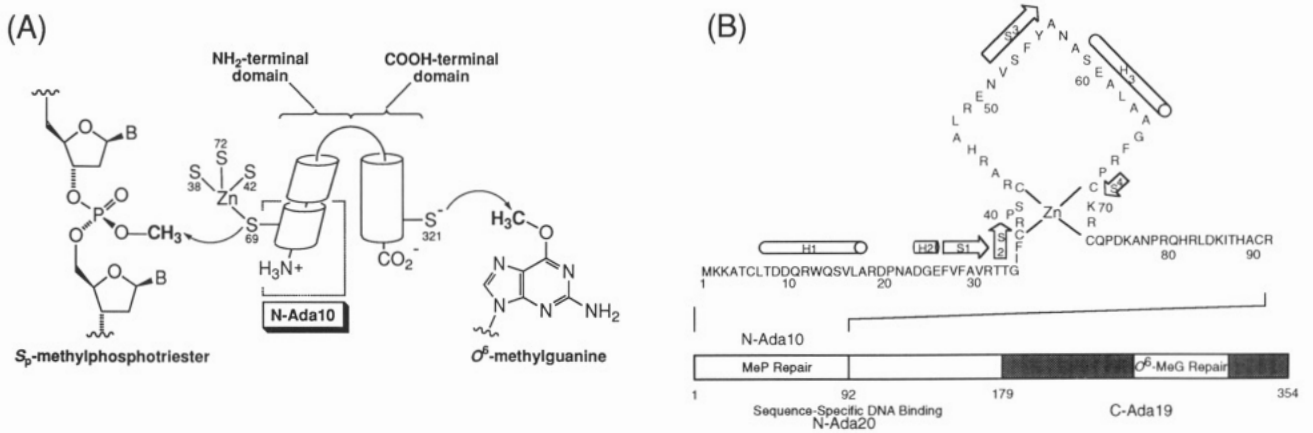


FIGURE 1: Schematics of the Ada protein, its constituent domains, its secondary structure, and a summary of Ada's DNA repair function. (A) Ada consists of two domains: the 20-kDa N-terminal domain (N-Ada20) repairs the $S_p$ diastereomer of methyl phosphotriesters and in the methylated form binds DNA sequence-specifically, while the 19-kDa C-terminal domain (C-Ada19) repairs the mutagenic lesion $O^6$-methylguanine by direct methyl transfer to Cys-321. Each domain retains its activity as an individual unit. The methyl phosphotriester repair and zinc-binding functionality are retained in the first 92 residues of the N-terminal N-Ada10. The metalloactivation of the methyl acceptor residue, Cys-69, is shown schematically. S refers to cysteine sulfhydryl groups of particular residues. (B) The domains of Ada and the sequence of N-Ada10. The zinc-binding site and a summary of the N-Ada10 secondary structure are shown within the sequence.

weiler & Ernst, 1983; Davis & Bax, 1985), homonuclear nuclear Overhauser effect spectroscopy (NOESY) (Jeener et al., 1979; Kumar et al., 1980), three-dimensional $^{15}$N-dispersed NOESY–heteronuclear multiple-quantum coherence (HMQC) spectroscopy (Fesik & Zuiderweg, 1988), double-quantum-filtered correlation spectroscopy (DQF-COSY) (Piantini et al., 1982; Müller et al., 1986) and $^{15}$N–$^{1}$H heteronuclear single-quantum coherence (HSQC) spectroscopy (Bodenhausen & Ruben, 1980) NMR spectra were recorded on a Bruker AMX-500 or AMX-600 spectrometer.

*Collection and Calibration of Restraints for Structure Calculations.* NOE-based interproton distance restraints were derived from two-dimensional (2D) NOESY and three-dimensional $^{15}$N-dispersed NOESY–HMQC spectra. Data were processed using Felix software. Upper distance limits of 5.0 and 4.5 Å were associated with the observation of NOESY cross-peaks at mixing times of 125 and 100 ms, respectively. For NOE cross-peaks observed in a 50-ms mixing time 2D NOESY spectrum, an integration and calibration technique (Hyberts et al., 1992) was used to quantify individual interproton distances. Intraresidue NOE-based distance restraints were used only if the cross-peak was quantified in the 50-ms NOESY. A 1.1-Å correction factor was added to NOE-based upper bounds involving methyl groups. Pseudo-atom corrections for phenyl ring protons and nonstereospecifically assigned methylene protons were made according to the reported protocol (Hyberts et al., 1992). Stereospecific assignments of all Val and Leu methyl groups as well as six $\beta$-methylene groups[2] were used in the NOE restraints. Dihedral restraints were used for both side-chain $\chi_1$ and backbone $\phi$ angles. The $\chi_1$ angle restraints were based on C$\alpha$H to C$\beta$H coupling constants obtained in a DQF-COSY, intraresidue NOE data and $^{15}$N to C$\beta$H coupling constants estimated from a $^{1}$H total correlation spectrum (TOCSY) on the $^{15}$N-labeled sample (Montelione et al., 1989). The $\chi_1$ dihedral restraints were assigned to one of the three staggered rotamer conformations (–60°, 180°, +60°) ± 60°. The $\phi$ dihedral restraints are based on estimated NH to C$\alpha$H coupling constants, obtained in a high-resolution $^{15}$N–$^{1}$H HSQC experiment and calibrated as previously reported (Kline et al., 1988). Slowly exchanging amide protons and NOE data implied the existence of 25 hydrogen bonds for which 50 distance restraints were included in the structure calculations. Drawing on $^{113}$Cd NMR data (Myers et al., 1993), a 2.3-Å thiol–zinc distance restraint was imposed on the four cysteine metal ligands. Additional distance and dihedral restraints were applied to enforce a tetrahedral metal ligation arrangement and to maintain proper sp$^3$ hybridization geometries of the coordinated sulfur atoms.

*Structure Calculation and Refinement.* DGII in the BIOSYM package was used to calculate structures by distance geometry methods. In this procedure, triangular inequality distance limits were determined by bounds smoothing. Randomized metrization was then used to determine random distance matrices that satisfy the triangular inequality distance limits. Coordinates with the appropriate distances were obtained and optimized by four-dimensional angular embedding and majorization procedures. The above generated structures were optimized in three dimensions by simulated annealing and conjugate gradient minimization (Havel, 1991). A total of 40 simulated annealing structures were calculated and 14 chosen for root-mean-square deviation (RMSD) analysis on the basis of lowest residual restraint violations. The ligand arrangement showed equal propensity to fall into the *S* or *R* configuration (Berg, 1988) in these calculations. To adopt the *R* configuration, however, would require unusual backbone $\phi$ angles and result in several strong NOEs that were not observed. Thus, calculated structures that resulted in the *R* configuration were eliminated from the analysis.

*Identification of Protein–DNA Substrate Interface.* A comparison of $^{1}$H–$^{15}$N HSQC spectra in the presence and absence of a double-stranded oligodeoxynucleotide was used to identify the interface between the protein and a DNA substrate utilized in MeP repair. An ≈0.15 molar equiv of the Dickerson dodecamer 5′d(CGCGAATTCGCG) was added to the $^{15}$N-labeled N-Ada10 sample. The criterion used to distinguish residues affected by interaction with the substrate was a change in backbone $^{1}$HN or $^{15}$N chemical shift [$\Delta > 0.05$ ppm ($^{1}$H) or $\Delta > 0.5$ ppm ($^{15}$N)] (Kallen et al., 1991). As a control, a $^{1}$H–$^{15}$N HSQC spectrum was taken after 500 mM NaCl was added to the protein–DNA mixture. The high-salt concentration should disrupt ionic contacts between the protein and the DNA, thereby causing the

[2] L. C. Myers, G. L. Verdine, and G. Wagner, unpublished results.

Table I: Summary of Structure Calculation Data

| restraint type | no. of restraints |
|---|---|
| all | 547 |
| interproton distances | |
| intraresidue | 108 |
| interresidue sequential ($\|i-j\| = 1$) | 175 |
| interresidue short range ($1 < \|i-j\| \leq 5$) | 91 |
| interresidue long range ($\|i-j\| > 5$) | 173 |
| hydrogen bond restraints | 50 |
| $Zn^{2+}$ distance restraints | 14 |
| dihedral angle restraints | 78 |

chemical shifts affected by the presence of the DNA to return to their original values.

## RESULTS

*Experimental Conformational Restraints.* Sequence-specific resonance assignments for the backbone and side chains of N-Ada10 were obtained using triple resonance experiments with an uniformly $^{13}C$,$^{15}N$-labeled sample, as well as standard methodology with $^{15}N$-labeled and unlabeled samples.[2] Using homonuclear 2D NOESY and $^{15}N$-dispersed three-dimensional NOESY spectra, 483 interesidue NOE connectivites have been identified in N-Ada10. Structures were generated using distance geometry methods (DGII) in the BIOSYM NMR Refine package on the basis of experimental distance and dihedral angle restraints. A summary of the structural statistics is shown in Table I. A complete list of distance and dihedral restraints has been submitted, along with the atomic coordinates, to the Brookhaven Protein Data Bank. The analysis of calculated structures is restricted to residues 8–73, since residues 1–7 and 74–92 appeared to form little well-defined secondary structure, as judged by their lack of medium- or long-range NOEs. The average RMSDs of the final 14 calculated structures from the mean coordinate positions are 0.92 ± 0.18 Å for the backbone atoms and 1.68 ± 0.21 Å for all heavy atoms. Residues 18–26 and 42–48 show few medium- or long-range NOEs and therefore are less well-defined than the rest of the protein backbone. Excluding these segments the RMSDs are 0.53 ± 0.07 Å for the backbone atoms and 1.29 ± 0.8 Å for all heavy atoms. The backbone RMSDs for N-Ada10 are much lower than the RMSDs which include all heavy atoms since a majority of the NOEs involve the backbone restraints, while there are few side-chain to side-chain restraints. This lack of observable side-chain NOEs results from the fact that a majority of the side chains are polar and reside on the surface of the protein while the core of the protein seems to be held together by a small number of hydrophobic interactions and the bound metal. None of the structures have NOE violations over 0.5 Å nor dihedral angle violations greater than 10°. Preliminary relaxation studies on N-Ada10 show that the lack of definition at the ends of the protein is due to high mobility and that the rest of the protein has fairly uniform dynamics, even in the less well-defined loops.[3]

*Structure of N-Ada10.* The global fold of N-Ada10 consists of a $\beta$-sheet sandwiched between two $\alpha$-helices (Figure 2). Ordered secondary structure (Figure 1B) in the protein begins with an $\alpha$-helix (H1), which makes several nonpolar contacts with the central $\beta$-sheet. A short $3_{10}$ helix (H2) comprising residues 23–27 leads into the central strand (S1) of a N-centered overhand three-stranded sheet (Richardson & Richardson, 1989). S1 is joined to the second antiparallel strand (S2) by a type I "common" turn (residues 32–35), while S2 is joined to the third antiparallel strand (S3) by a loop (residues 42–48), which shows few long-range NOEs with the sheet. S3 leads into the second $\alpha$-helix (H3), which also makes several nonpolar contacts with the N-centered sheet. H3 leads into a fourth strand (S4), which is joined to S2 in a parallel orientation. The overall fold of N-Ada10 is unrelated to any protein of known structure, as speculated on the basis of modeling studies (Swindells, 1993).

*Zinc-Binding Motif of Ada.* The zinc-binding pocket of N-Ada10 lies on the edge of the $\beta$-sheet and is formed by the two parallel strands of the $\beta$-sheet and the loops that extend from each (Figure 2C). The zinc in Ada is tetrahedrally coordinated to four cysteine residues (Cys-38, -42, -69, -72), as previously suggested on the basis of sequence conservation (Myers et al., 1992) and $^{113}Cd$ NMR experiments (Myers, 1993). These same four residues and no other potential ligands converged on the same region of three-dimensional space, even when explicit restraints for ligation to zinc were not imposed. The active site residue and zinc ligand, Cys-69, is on the solvent-exposed edge of the short segment of parallel sheet, positioned directly across the sheet from another metal ligand, Cys-38 (Figure 2C). The other two ligands are present on roughly parallel loop structures.

The higher degree of structural uncertainty associated with the metal binding loops of N-Ada10, compared to the central core of the protein, is a result of a lower number of available restraints per residue rather than an effect of mobility[3] and is not unique to Ada. A high-resolution NMR structure of calbindin also showed high RMSD values with the absence of high mobility in the protein's solvent-exposed metal binding loops (Kördel et al., 1992).

*Comparison of Ada with Other Zinc-Binding Proteins.* Notwithstanding the higher degree of structural uncertainty in the metal binding loops, the N-Ada10 zinc-binding motif is clearly distinct from other structurally characterized proteins that utilize four cysteine ligand arrangements: alcohol dehydrogenase (ADH), aspartate transcarbamoylase (ATCase) (Vallee & Auld, 1990), or most notably the nuclear hormone receptor class of transcription factors (Schwabe & Rhodes, 1991). Like ADH and ATCase, however, the zinc in Ada is not integral to the core of the protein but appears to maintain the local structure in the immediate vicinity of the metal.

*Analysis of N-Ada10-DNA Substrate Interface.* To characterize the nonspecific interactions utilized in DNA MeP repair, amide backbone cross-peaks in a $^{1}H$–$^{15}N$ HSQC spectrum were examined in the presence of a 12-mer duplex oligodeoxynucleotide. Identification of protein moieties involved in DNA contacts was based on a change in backbone $^{1}HN$ and $^{15}N$ resonance positions upon addition of DNA. Significant chemical shift differences are observed for only four residues of N-Ada10 (Figure 2D), indicating little conformational change in the presence of DNA. The residues that met the chemical shift criteria were Arg-43, Arg-45, Leu-48, and Cys-69. The largest observed changes in chemical shift were $\Delta$ = 0.1 ppm ($^{1}H$) and $\Delta$ = 1.2 ppm ($^{15}N$) for Arg-45. Upon addition of high salt (500 mM) the affected chemical shifts returned to the positions observed in the absence of DNA.

## DISCUSSION

Earlier studies on Ada revealed that ionic zinc or cadmium was necessary for the proper folding of the N-terminal domain (Myers et al., 1992). Furthermore, mutation of the active site ligand, Cys-69, to noncoordinating residues such as Ala

[3] J. Habazettl, L. C. Myers, G. L. Verdine, and G. Wagner, unpublished results.

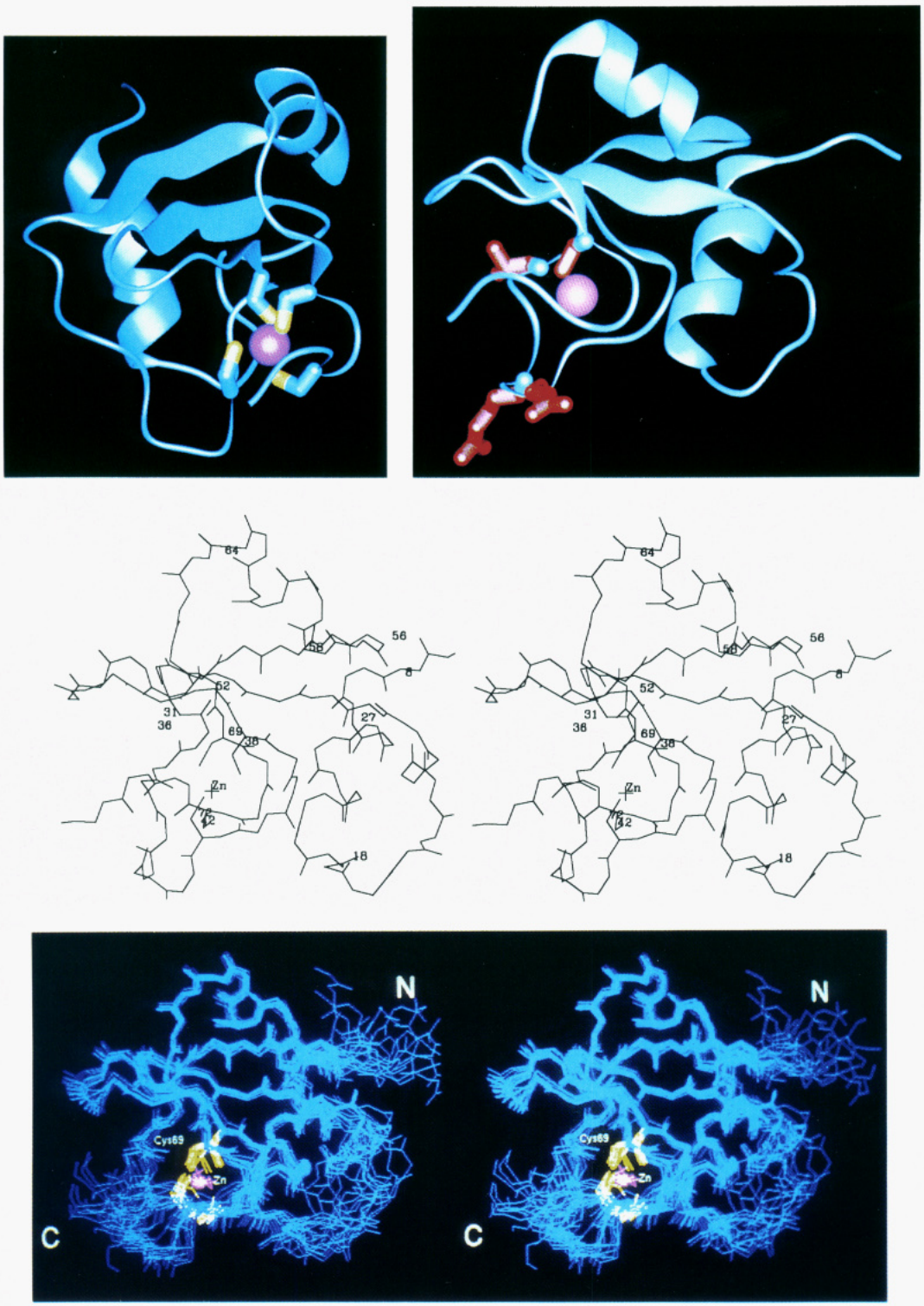


FIGURE 2: Structure of N-Ada10. (A, top) Stereoview of the overlay of 14 final structures of N-Ada10 (residues 5–75). All backbone heavy atoms are shown in light blue. The zinc-binding cysteine side chains are yellow, and the zinc atom itself is marked by a magenta cross. The proximal N- and C-termini are labeled N and C, respectively. (B, middle) Stereoview of the N-Ada10 structure having the smallest RMSD backbone difference with the average structure. All backbone heavy atoms (residues 5–75) are shown, as are the side chains of the four zinc ligand residues and the zinc ion. Reference numbers are displayed for the zinc ligand cysteine residues and key points in the secondary structure of N-Ada10. (C, bottom left) Ribbon trace of the N-Ada10 structure showing the zinc-binding motif. The orientation shown is rotated ≈90° about the *Z* axis with respect to panels A and panel B. The backbone and side-chain carbons are displayed in blue, the cysteine sulfurs are in yellow, and the zinc atom is in magenta. The zinc-binding cysteines are, clockwise from the upper left, Cys-38, Cys-69, Cys-72, and Cys-42. (D, bottom right) Ribbon trace of the N-Ada10 structure depicting in red side chains of residues that show a change in amide $^{15}N$ or $^{1}HN$ chemical shifts after the addition of a 12-mer duplex Oligodeoxynucleotide. Clockwise from the upper left these residues are Leu-48, Cys-69, Arg-43, and Arg-45.

or Ser produced Ada variants that folded poorly;[4] on the other hand, the mutant protein having His at position 69, which has been shown to coordinate zinc, folds as wild type (Myers et al., 1993). The structure of the N-terminal zinc-binding domain sheds some light on these observations. Although much of the central protein core forms a widely observed

[4] M. P. Terranova, L. C. Myers, and G. L. Verdine, unpublished results.

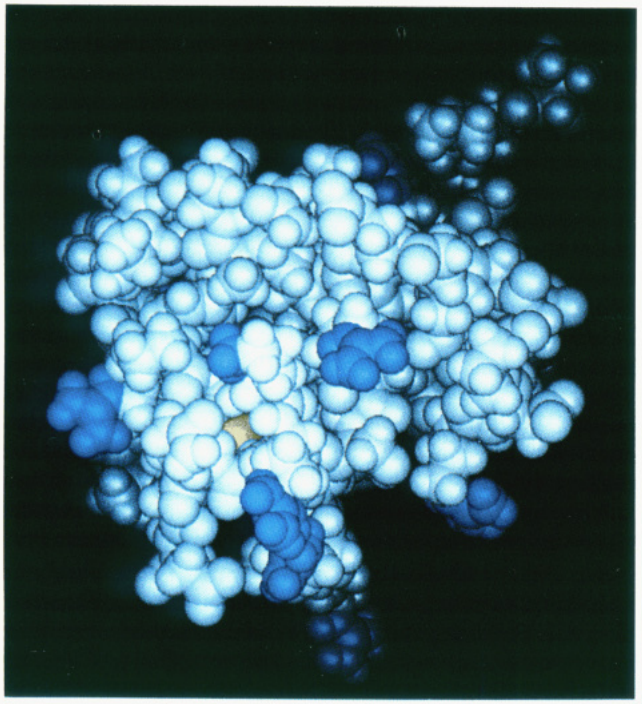

FIGURE 3: Potential substrate binding surface of N-Ada10 visualized with space-filling molecular models. The orientation shown is identical with that shown in Figure 2A,B,D. N-Ada10 is shown in gray, except that charged atoms on basic residues are in blue and the sulfur of Cys-69 is in yellow.

topology, namely, an N-centered overhand three-stranded sheet, the crossover from the third antiparallel strand (S3) to the short parallel strand (S4), which contains Cys-69, is an unusual topology where the parallel strand appears to be stabilized largely by ligation to the metal. Apart from metal ligation there appear to be few interactions, such as the nonpolar side-chain interactions that help stabilize the antiparallel sheet, to stabilize the parallel $\beta$-strands and the loops emanating from them. It could readily be envisioned that loss of metal ligation at position 69 could peel away the short parallel strand (S4) from the central sheet, thereby destabilizing the protein. Thus, the structure demonstrates the critical importance of zinc in stabilizing the overall fold of N-Ada10 and in particular the tertiary structure of the active site.

The identification of Cys-69 as a ligand residue of Ada implicated the zinc ion not only in stabilization of the protein structure but also in direct metalloactivation of the methyl acceptor residue (Myers et al., 1993). Presumably, coordination of Cys-69 to the metal destabilizes (acidifies) the thiol form and stabilizes the corresponding thiolate. This mode of activation is unusual among proteins that possess nucleophilic Cys residues, such as thymidylate synthase (Matthews et al., 1990) and papain (Johnson et al., 1981a–c). In these enzymes, interaction of a Cys residue with a basic amino acid results in proton transfer, with the thiolate being stabilized through ion pairing. Ada does not have access to such a mechanism, since none of the basic residues near Cys-69 are close enough to deprotonate it (Figure 3). Although unusual in protein chemistry, the ability of metals to enhance the reactivity of thiol groups toward electrophiles is well precedented in small molecule coordination complexes (Lindoy & Busch, 1974; Elder et al., 1978; Rajanikanth & Ravindranath, 1984); the nucleophilic species in such reactions is known to be the metal-bound thiolate, as opposed to a thiolate that has transiently dissociated from the metal (Jadmus et al., 1964). Hence, coordination of a thiolate to zinc does not protect it from electrophilic attack but rather increases its tendency to react. Ada thus exhibits the intrinsic chemistry of zinc-bound thiolates, while positioning the substrate to direct methyl transfer specifically to Cys-69. Evidence for metalloactivation of a zinc-bound thiolate toward electrophilic chemical reagents has also been reported in the case of matrix metalloproteases (Springman et al., 1990). Other proteins that possess zinc-bound thiolates may be designed to suppress their intrinsic reactivity. Hydrogen bonds to the coordinated sulfur atoms observed in several proteins (Blake & Summers, 1993), mainly from backbone amide protons, can serve to decrease the negative charge density on the ligand and thereby decrease its nucleophilicity. The N-Ada10 structure suggests the protein may possess no such interactions: the distances and relative orientations of amide protons and sulfur atoms in the ensemble of structures, and the lack of slowly exchanging amide protons in the residues near the sulfur atoms, are both inconsistent with the presence of hydrogen bonds.

The N-Ada10 structure reveals that Cys-69 is embedded in a solvent-exposed surface of the protein where it is accessible to outside approach (Figures 2C, 3). Conserved basic residues (Hakura et al., 1991) on the solvent-exposed surface (Arg-39, Arg-43, Arg-45, Arg-67, Lys-70, and Arg-71) presumably form nonspecific electrostatic interactions with the negatively charged DNA phosphodiester backbone to orient the protein and its substrate. Two of these basic residues, Arg-43 and Arg-45, are among the four residues which show significant changes in chemical shift upon addition of a nonspecific DNA substrate. These four residues which show changes in chemical shift, including the active site residue Cys-69, define a reasonable substrate interface for MeP repair (Figure 2D).

The stereospecific nature of Ada's DNA MeP repair process appears to arise in part from steric constraints imposed on both the protein and DNA. For regular B-form DNA the $S_p$ MeP diastereomer projects directly out into solution from the edge of the phosphodiester backbone, whereas the $R_p$ diastereomer projects inward toward the major groove. Because the active site thiolate is embedded in the surface of the protein, it is inaccessible to the more sterically inaccessible $R_p$ MeP diastereomer. Consistent with this analysis, simple model building studies (not shown) suggested that the necessary proximity and alignment for nucleophilic attack could only be achieved for the $S_p$ diastereomer. The negative charge that develops in the transition state on the phosphate oxygens may be stabilized by electrostatic interactions with basic residues or hydrogen bonds to backbone or side-chain amide protons. N-Ada10 repairs MeP at the same rate as Ada and N-Ada20 but does not bind DNA sequence-specifically.[5] Consistent with this finding, there appears to be no element in the solution structure of N-Ada10 indicative of a sequence-specific DNA binding domain. Hence, residues in the stretch from 75 to 146 (Sakashita et al., 1993) must form such DNA binding elements. It remains to be determined how methylation of Cys-69, a zinc ligand, is connected to the sequence-specific DNA binding element.

The phosphotriester repair domain of Ada possesses a novel structure that is uniquely suited to promote metalloactivated demethylation of MeP. Although the reaction carried out by Ada is necessarily autocatalytic, we have speculated that catalytic versions of the same reaction might exist (Myers et al., 1993). Indeed, recent evidence suggests that a reactive Cys residue in the p21$^{Hras}$ protein, part of a CXAA motif that

[5] F. Jackow, L. C. Myers, and G. L. Verdine, unpublished results.

is S-alkylated by farnesyl pyrophosphate, may require coordination to a zinc ion bound by the farnesyltransferase enzyme (Reiss et al., 1992).

## ACKNOWLEDGMENT

We thank R. Clubb, K. Chandrasekhar, and V. Thanabal for assistance with the spectroscopy and A. Krezel and J. Withka for discussions on structure determination. We also thank S. Wolfe for providing the Dickerson dodecamer sample.

## SUPPLEMENTARY MATERIAL AVAILABLE

Figure 1S showing a composite HNCA spectrum used in the sequence-specific assignment of the N-Ada10 resonances, Figure 2S showing the aliphatic proton region of a 2D NOESY spectrum performed in $D_2O$, and Figure 3S showing the NOE statistics by residue for the structure calculation on N-Ada10 (5 pages). Ordering information is given on any current masthead page.

## REFERENCES

Berg, J. M. (1988) *Proc. Natl. Acad. Sci. U.S.A. 85*, 99–102.
Berg, J. M. (1990) *J. Biol. Chem. 265*, 6513–6516.
Blake, P. R., & Summers, M. F. (1993) *Adv. Biophys. Chem.* (in press).
Bodenhausen, G., & Ruben, D. J. (1980) *Chem. Phys. Lett. 69*, 185–199.
Braunschweiler, L., & Ernst, R. R. (1983) *J. Magn. Reson. 53*, 521–528.
Davis, D. G., & Bax, A. (1985) *J. Am. Chem. Soc. 107*, 2820–2821.
Demple, B. (1990) in *Protein Methylation* (Paik, W. K., & Kim, S., Eds.) pp 285–304, CRC Press, Boca Raton, FL.
Elder, R. C., Kennard, G. J., Payne, M. D., & Deutsch, E. (1978) *Inorg. Chem. 17*, 1296–1303.
Fesik, S. W., & Zuiderweg, E. R. P. (1988) *J. Magn. Reson. 78*, 588–593.
Hakura, A., Morimoto, K., Sofuni, T., & Nohmi, T. (1991) *J. Bacteriol. 173*, 3663–3672.
Havel, T. F. (1991) *Prog. Biophys. Mol. Biol. 56*, 43–78.
Hyberts, S. G., Goldberg, M. S., Havel, T. F., & Wagner, G. (1992) *Protein Sci. 1*, 736–751.
Jadmus, H., Fernando, Q., & Freiser, H. (1964) *J. Am. Chem. Soc. 86*, 3056–3059.
Jeener, J., Meier, B. H., Bachmann, P., & Ersnt, R. R. (1979) *J. Chem. Phys. 71*, 4546–4553.
Johnson, F. A., Lewis, S. D., & Schafer, J. A. (1981a) *Biochemistry 20*, 44–47.
Johnson, F. A., Lewis, S. D., & Schafer, J. A. (1981b) *Biochemistry 20*, 48–51.
Johnson, F. A., Lewis, S. D., & Schafer, J. A. (1981c) *Biochemistry 20*, 52–55.
Kallen, J., Spitzfaden, C., Zurini, M. G. M., Wider, G., Widmer, H., Wüthrich, K., & Walkinshaw, M. D. (1991) *Nature 353*, 276–279.
Kline, A. D., Braun, W., & Wüthrich, K. (1988) *J. Mol. Biol. 204*, 675–724.
Kördel, J., Skelton, N. J., Akke, M., Palmer, A. G., & Chazin, W. (1992) *Biochemistry 31*, 4856–4866.
Kumar, A., Ernst, R. R., & Wüthrich, K. (1980) *Biochem. Biophys. Res. Commun. 95*, 1–6.
Lindahl, T. (1993) *Nature 362*, 709–715.
Lindahl, T., Sedgewick, B., Sekiguchi, M., & Nakabeppu, Y. (1988) *Annu. Rev. Biochem. 57*, 133–157.
Lindoy, L. F., & Busch, D. H. (1974) *Inorg. Chem. 13*, 2494–2498.
Matthews, D. A., Villafranca, J. E., Janson, C. A., Smith, W. W., Welsh, K., & Freer, S. (1990) *J. Mol. Biol. 214*, 937–948.
Montelione, G. T., Winkler, M. E., Rauenbuehler, P., & Wagner, G. (1989) *J. Magn. Reson. 82*, 198–204.
Müller, N., Ernst, R. R., & Wüthrich, K. (1986) *J. Am. Chem. Soc. 108*, 6482–6492.
Myers, L. C., Terranova, M. P., Nash, H. M., Markus, M. A., & Verdine, G. L. (1992) *Biochemistry 31*, 4541–4547.
Myers, L. C., Terranova, M. P., Ferentz, A. E., Wagner, G., & Verdine, G. L. (1993) *Science 261*, 1164–1167.
Piantini, U., Sørensen, O. W., & Ernst, R. R. (1982) *J. Am. Chem. Soc. 104*, 6800–6801.
Rajanikanth, B., & Ravindranath, B. (1984) *Indian J. Chem. 23B*, 1043–1045.
Reiss, Y., Brown, M. S., & Goldstein, J. L. (1992) *J. Biol. Chem. 267*, 6403–6408.
Richardson, J. S., & Richardson, D. C. (1989) in *Prediction of Protein Structure and the Principles of Protein Conformation* (Fasman, G. D., Ed.) pp 1–98, Plenum, New York.
Sakashita, H., Sakuma, T., Ohkubo, T., Kainosho, M., Sakumi, K., Sekiguchi, M., & Morikawa, K. (1993) *FEBS Lett. 323*, 252–256.
Schwabe, J. W. R., & Rhodes, D. (1991) *Trends Biochem. Sci. 16*, 291–296.
Springman, E. B., Angleton, E. L., Birkedal-Hansen, H., & Van Wart, H. E. (1990) *Proc. Natl. Acad. Sci. U.S.A. 87*, 364–368.
Swindells, M. B. (1993) *FEBS Lett. 323*, 257–260.
Vallee, B. L., & Auld, D. S. (1990) *Biochemistry 29*, 5647–5659.